Aerospace Science and Technology 55 (2016) 264–271

Contents lists available at ScienceDirect

Aerospace Science and Technology

www.elsevier.com/locate/aescte

Airplane loss of control problem: Linear controllability analysis

Ahmed M. Hassan [*,1], Haithem E. Taha [2]

University of California, Irvine, CA 92697, United States

ARTICLE INFO

Article history:
Received 17 January 2016
Received in revised form 29 April 2016
Accepted 1 June 2016
Available online 3 June 2016

Keywords:
Airplane controllability
Airplane loss-of-control
Landing-approach
Thrust-only flight control systems

ABSTRACT

The controllability analysis for airplane flight dynamics is very crucial in upset/loss-of-control situations. Conventional airplanes are normally equipped with so redundant control authority. That is, an airplane might experience a loss of one or more control surfaces and remain controllable. As such, the aim of this paper is to investigate common upset situations and to explore the limits of controllability using linear analysis tools with emphasis on analysis of Thrust-only Flight Control Systems (TFCSs) where all the hydraulic systems are lost. Based on those analyses, the necessity of nonlinear controllability analysis for such situations is discussed.

1. Introduction

Control loss of an airplane, known in literature as loss-of-control, is a serious problem whose repercussions can be catastrophic. Luckily, conventional airplanes may still be controllable if one or more control surfaces fail. For example, if an airplane lost all of its control surfaces due to hydraulic failure, it may still be controllable by manipulating the engines thrust forces. There are two common incidents in history that support such a fact. In 1989, the United Airlines Flight 232 DC-10 aircraft lost flight control surfaces due to hydraulic pressure loss because of a failure in its tail-mounted engine. However, the crew managed to control the airplane until they reached an airport. Nevertheless, the aircraft lost balance just before touchdown leading to a wing-tip crash into the run way, which in turn, led to the aircraft breaking apart. But 185 people survived out of the 296 on board. The 2003 DHL A300-B4 aircraft incident is another example. The aircraft was hit by a ground-to-air missile during initial climb right after takeoff from Baghdad airport. As such, all hydraulics were lost within few seconds. However, the crew managed to land the airplane safely using only thrust controls. Of course, there are other examples of flight control failures where the crew could not avoid the worst case scenario such as the 1974 Turkish Airlines Flight 981. The DC-10 aircraft lost the cargo door, which leads to a damage in the control cables. The aircraft crashed a minute later and none of the 346 people on board survived.

The above incidents among others invoked design and analysis of a thrust-only flight control system (TFCS) or a propulsion controlled aircraft (PCA). These systems have been investigated in the 1990s by Burcham et al. [5,6] and Tucker [20] at NASA Dryden Flight Research Center. They developed a computer-assisted engine control system, implemented and tested it on the F-15 fighter aircraft and the MD-11 transport aircraft. In his study of the 2003 DHL A300-B4 aircraft incident, Lemaignan [13] analyzed the applicability of TFCSs. More recently, Yamasaki et al. [22], at Mitsubishi Heavy Industries, developed a TFCS system for the Boeing 747-400 and validated it by testing in a domed simulator.

On the other hand, Wilborn and Foster [21], at Boeing Company and NASA Langley Research Center, presented a quantitative measures for loss-of-control in commercial transport aircraft. They presented five envelopes relating to airplane flight dynamics, aerodynamics, structural integrity, and flight control use that can reliably identify key Loss-of-control characteristics. Also, Kwatny et al. [12] presented a nonlinear analysis for aircraft loss-of-control. They examined the ability to regulate an aircraft around stall points with emphasis on impaired aircraft and presented some examples using NASA's generic transport model.

The objective of this paper is to formulate the airplane loss of control (LOC) into a controllability framework. It is understandable that controllability of a linearized model is not necessary. That is there exists a class of systems that are linearly uncontrollable but nonlinearly controllable, see for example Sec. 3.1 in Ref. [17]. However, the linear analysis should be performed first because of its sufficiency. Then nonlinear analysis should be employed in the cases where the linear analysis fails. Therefore, the current effort is to perform linear controllability analysis for some LOC cases (e.g., no elevator) and identify situations where nonlinear analysis

* Corresponding author.
E-mail addresses: ahmedmh@uci.edu (A.M. Hassan), hetaha@uci.edu (H.E. Taha).
[1] Ph.D. Student, Mechanical and Aerospace Engineering, Engineering Gateway.
[2] Assistant Professor, Henry Samueli Career Development Chair, Mechanical and Aerospace Engineering, Engineering Gateway.

http://dx.doi.org/10.1016/j.ast.2016.06.001
1270-9638/

is required. A successive effort will be to discuss nonlinear controllability and apply it to these situations.

In this work, a linear decoupled six-degrees-of-freedom flight dynamic model is considered. Controllability of the linearized model about the cruise equilibrium is assessed at no-elevator, no-aileron, no-rudder, and no-thrust situations. In particular, the landing-approach problem using TFCS is analyzed. Also, the concerns raised by Lemaignan [13] and Nguyen et al. [16] are addressed. Finally, LOC situations that necessitate nonlinear controllability analysis are provided for a successive effort.

2. Linear controllability analysis

Controllability is defined as the ability to steer a given system from some configuration into another configuration in finite time. A linear time-invariant (LTI) system is written in the form

$$\dot{\boldsymbol{x}}(t) = \boldsymbol{A}\boldsymbol{x}(t) + \boldsymbol{B}\boldsymbol{u}(t) \tag{1}$$

where $\boldsymbol{x}$ is the state vector $(n \times 1)$, $\boldsymbol{u}$ is the control input vector $(m \times 1)$, $\boldsymbol{A}$ is the state matrix $(n \times n)$, and $\boldsymbol{B}$ is the input matrix $(n \times m)$. A necessary and sufficient condition for the controllability of the system (1) is that the $(n \times nm)$ controllability matrix

$$\boldsymbol{C} = \begin{bmatrix} \boldsymbol{B} & \boldsymbol{A}\boldsymbol{B} & \boldsymbol{A}^2\boldsymbol{B} & \dots & \boldsymbol{A}^{n-1}\boldsymbol{B} \end{bmatrix} \tag{2}$$

to be of full rank (i.e. $\text{rank}(\boldsymbol{C}) = n$) which is often denoted by Kalman rank condition [18].

Luckily, controllability of linear systems is constructive. That is, if the matrix $\boldsymbol{C}$ is of full rank, then the following relation provides a control input history that steers the system (1) from $\boldsymbol{x}_0$ at t_0 to $\boldsymbol{x}_1$ at t_1 [3, pp. 74–77]

$$\begin{aligned} \boldsymbol{u}(t) &= -\boldsymbol{B}'\,\boldsymbol{\Phi}'(t_0,t)\,\boldsymbol{W}^{-1}(t_0,t_1)\,\big(\boldsymbol{x}_0 - \boldsymbol{\Phi}(t_0,t_1)\,\boldsymbol{x}_1\big) \\ \boldsymbol{W}(t_0,t_1) &= \int_{t_0}^{t_1} \boldsymbol{\Phi}(t_0,t)\,\boldsymbol{B}\,\boldsymbol{B}'\,\boldsymbol{\Phi}'(t_0,t)\,dt \end{aligned} \tag{3}$$

where $(.)'$ denotes the transpose, $\boldsymbol{\Phi}$ is the state transition matrix which is defined as $\Phi(t_0,t) = e^{\boldsymbol{A}(t_0-t)}$. It should be noted that the control law (3) minimizes the integral $\int_{t_0}^{t_1} ||\boldsymbol{u}(t)||^2 dt$ of control energy needed for steering.

On the other hand, for nonlinear, control-affine system in the form

$$\dot{\boldsymbol{x}} = \boldsymbol{f}(\boldsymbol{x}) + \sum_{i=1}^{m} \boldsymbol{g_i}(\boldsymbol{x}) u_i \tag{4}$$

where $\boldsymbol{f}(\boldsymbol{x})$ is the drift vector field (uncontrolled dynamics) and $\boldsymbol{g_i}(\boldsymbol{x})$ is the control input vector field associated with the control input u_i. Assume, without loss of generality, that $\boldsymbol{x}_0$ is an equilibrium point (i.e. $\boldsymbol{f}(\boldsymbol{x}_0) = 0$). A sufficient condition for the local controllability of the system (4) at $\boldsymbol{x}_0$ is that the linearization about $\boldsymbol{x}_0$, written as

$$\Delta\dot{\boldsymbol{x}} = \left[\frac{\partial \boldsymbol{f}}{\partial \boldsymbol{x}}\right]\bigg|_{\boldsymbol{x}_0} \Delta\boldsymbol{x} + \sum_{i=1}^{m} \boldsymbol{g_i}(\boldsymbol{x}_0) u_i \tag{5}$$

to be controllable. That is, the controllability matrix

$$\begin{aligned} \boldsymbol{C} = \Bigg[& \boldsymbol{g_1}(\boldsymbol{x}_0), \dots, \boldsymbol{g_m}(\boldsymbol{x}_0), \left[\frac{\partial \boldsymbol{f}}{\partial \boldsymbol{x}}\right]\bigg|_{\boldsymbol{x}_0} \boldsymbol{g_1}(\boldsymbol{x}_0), \dots, \left[\frac{\partial \boldsymbol{f}}{\partial \boldsymbol{x}}\right]\bigg|_{\boldsymbol{x}_0} \boldsymbol{g_m}(\boldsymbol{x}_0), \dots \\ & \dots, \left[\frac{\partial \boldsymbol{f}}{\partial \boldsymbol{x}}\right]^{n-1}\bigg|_{\boldsymbol{x}_0} \boldsymbol{g_1}(\boldsymbol{x}_0), \dots, \left[\frac{\partial \boldsymbol{f}}{\partial \boldsymbol{x}}\right]^{n-1}\bigg|_{\boldsymbol{x}_0} \boldsymbol{g_m}(\boldsymbol{x}_0) \Bigg] \end{aligned} \tag{6}$$

to be of full row rank [17]. It is noteworthy to mention that this controllability matrix of the linearized system (5) is the analogue of the controllability matrix of the linear system (1), where $\left[\frac{\partial \boldsymbol{f}}{\partial \boldsymbol{x}}\right]\Big|_{\boldsymbol{x}_0}$ is the Jacobian matrix of the vector field $\boldsymbol{f}(\boldsymbol{x})$ evaluated at $\boldsymbol{x}_0$, which is equivalent to the matrix A in (1) and $[\boldsymbol{g_1}(\boldsymbol{x}_0), \dots, \boldsymbol{g_m}(\boldsymbol{x}_0)]$ is equivalent to the matrix B in (1).

3. Controllability analysis of linearized flight dynamics

In this section, the controllability analysis of the linearized system is performed. Since this linearization is performed at the cruise flight condition; i.e., the lateral velocity $v = 0$ as well as the rolling and yawing angular velocities $p = r = 0$, then the longitudinal and lateral dynamics are decoupled and their respective reduced-order models can be studied separately.

3.1. Longitudinal 4×4 flight dynamics model

The longitudinal 4×4 flight dynamics model for a rigid aircraft can be written as follows [15]

$$\begin{aligned} \begin{bmatrix} \dot{u} \\ \dot{w} \\ \dot{q} \\ \dot{\theta} \end{bmatrix} &= \begin{bmatrix} X_u & X_w & 0 & -g\cos\theta_0 \\ Z_u & Z_w & U_0 & -g\sin\theta_0 \\ M_u & M_w & M_q & -gM_w\sin\theta_0 \\ 0 & 0 & 1 & 0 \end{bmatrix} \begin{bmatrix} u \\ w \\ q \\ \theta \end{bmatrix} \\ &\quad + \begin{bmatrix} X_{\delta_e} & X_{\delta_t} \\ Z_{\delta_e} & 0 \\ M_{\delta_e} & M_{\delta_t} \\ 0 & 0 \end{bmatrix} \begin{bmatrix} \delta_e \\ \delta_t \end{bmatrix} \end{aligned} \tag{7}$$

where u and w are the forward and normal velocity perturbations of the airplane center of gravity from the equilibrium state along the longitudinal and normal body axes, respectively. The body pitching angle and angular velocity are θ and q, respectively. U_0 and θ_0 are the cruise forward speed and pitching angle, respectively and g is the gravitational acceleration. The longitudinal control inputs are the elevator deflection δ_e and thrust control input δ_t. The parameters X_u, X_w, Z_u, Z_w, M_u, M_w, M_q, X_{δ_e}, X_{δ_t}, Z_{δ_e}, M_{δ_e}, and M_{δ_t} are stability and control derivatives at the cruise condition.

The rank of the controllability matrix for this system is calculated using Eq. (2) and found to be **four** which ensures linear (and hence nonlinear) controllability for the system at hand. In case of a failure in the elevator system or loss of regulation in the engine system, the control input matrix $\boldsymbol{B}$ becomes $[X_{\delta_t}\ 0\ M_{\delta_t}\ 0]'$ or $[X_{\delta_e}\ Z_{\delta_e}\ M_{\delta_e}\ 0]'$, respectively. However, in either case, the rank of the controllability matrix is found to be also **four**, which means that the airplane remains controllable even if the elevator or engine fails.

In order to verify the existence of a steering control input history in the case of elevator or engine loss, we use the longitudinal flight dynamic characteristics of the DELTA aircraft (a paradigm model for a very large, four-engined, cargo jet aircraft) from [14, pp. 561–563], at the flight condition (sea-level cruising at $U_0 = 75$ m/s and $\theta_0 = \alpha_0 = 2.7°$). It is preferred over a particular airplane type (e.g., B747, A320) for its general representation for a whole class of airplanes. However, it should be noted that the presented analysis is transferable to any class. The stability and control derivatives of such an airplane at the stated flight condition are given as:

$$\begin{aligned} & m = 300{,}000\ \text{kg},\ X_u = -0.02,\ X_w = 0.1, \\ & Z_u = -0.23,\ Z_w = -0.634, \\ & M_u = -2.55 * 10^{-5},\ M_w = -0.005,\ M_q = -0.61, \\ & X_{\delta_e} = 0.14,\ Z_{\delta_e} = -2.9, \\ & M_{\delta_e} = -0.64,\ X_{\delta_t} = 1.56,\ M_{\delta_t} = 0.0054. \end{aligned}$$

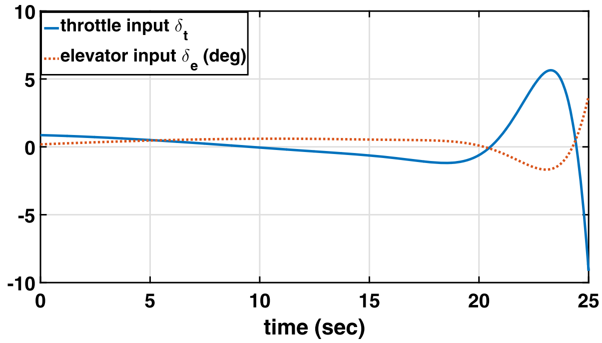

Fig. 1. Control input history for DELTA aircraft to reach $\boldsymbol{x}_1 = [80 \quad 0 \quad 0 \quad 3.7°]'$.

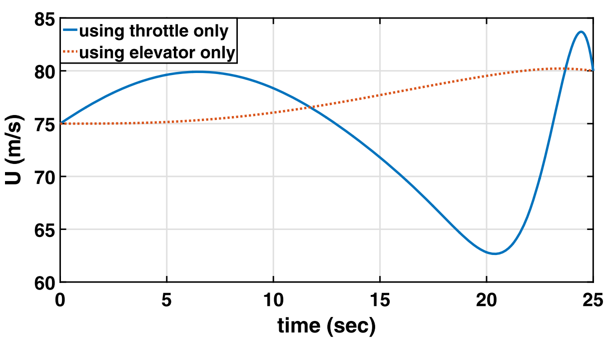

Fig. 2. Variation of the body velocity U for DELTA aircraft model due to the control input shown in Fig. 1.

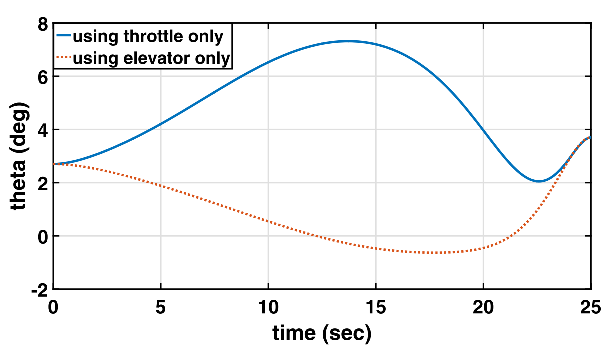

Fig. 3. Variation of the pitch angle θ for DELTA aircraft model due to the control input shown in Fig. 1.

where X_{δ_t} is calculated as $X_{\delta_t} = \frac{T_{max} - T_{trim}}{m}$, T_{max} is the max allowable thrust for this airplane and it is given to be 730 KN, and T_{trim} is the thrust trim value which is calculated, using the drag polar relation, at this flight condition to be 262 KN, in this way the allowed δ_t should be between 1 and -0.56. The control derivative M_{δ_t} is calculated based on the assumption that the thrust line has an offset of 0.5 m below the center of gravity line.

Now, we use the minimal control energy input presented in Eq. (3) to calculate a control input history to attain a final state $\boldsymbol{x}_1 = [80 \quad 0 \quad 0 \quad 3.7°]'$. Figs. 1–4 show the control input history to reach the state $\boldsymbol{x}_1$ over the course of 25 seconds, the resulting forward velocity U, the resulting pitch angle θ, and the vertical trajectory respectively. Obviously, the throttle control input exceeds the control input bounds, but this is not of a concern here. At this point, we are just concerned about the existence of a steering control input history. A control input history that is confined to the control input bounds could be designed using an optimal control approach (e.g., Linear Quadratic Regulator) as will be shown in the subsequent sections.

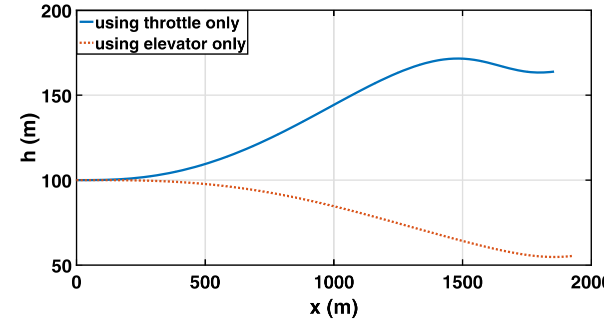

Fig. 4. Vertical Trajectory for DELTA aircraft model due to the control input shown in Fig. 1.

It should be noted that even if $M_{\delta_t} = 0$, the linear controllability of the system is still preserved using the thrust control only due to the indirect pitch control authority via speed regulation. That is, thrust manipulations induce velocity changes, which in turn induces a change in the pitching moment. This point will also be discussed further in Sec. 4.2.1.

It is noteworthy to emphasize the fact that linear controllability implies reachability in the sense that any arbitrarily given state can be reached in arbitrary time with unbounded controls and in finite time with control bounds. However, the system may depart from such a state immediately after the excursion time. In other words, controllability does not necessarily imply equilibrium, as the latter necessitates forcing to sustain. As such, it is not surprising that the controllability of the fourth order longitudinal model is preserved even if one longitudinal control input is removed. There will be always a control strategy that steers the longitudinal flight dynamics to a given final state, making use of the available potential energy. As shown in Fig. 4, the airplane lost altitude in order to reach the desired final state, because no restriction is imposed on the final altitude. As such, for a more representative analysis, the altitude should be included as a state, as shown in the next subsection.

3.2. *Longitudinal* 5×5 *flight dynamics model*

During the landing-flare phase, the altitude should follow a certain temporal trajectory [2, pp. 94–97]. As such, linear controllability of the longitudinal flight dynamics, including the altitude as a state variable, must be ensured. In this subsection, the altitude state h is included in the longitudinal flight dynamics model and the controllability of the system is assessed again in various situations. Firstly, the linearized longitudinal flight dynamics model is then written as

$$\begin{bmatrix} \dot{u} \\ \dot{w} \\ \dot{q} \\ \dot{\theta} \\ \dot{h} \end{bmatrix} = \begin{bmatrix} X_u & X_w & 0 & -g\cos\theta_0 & 0 \\ Z_u & Z_w & U_0 & -g\sin\theta_0 & 0 \\ M_u & M_w & M_q & -gM_w\sin\theta_0 & 0 \\ 0 & 0 & 1 & 0 & 0 \\ \sin\theta_0 & -\cos\theta_0 & 0 & U_0\cos\theta_0 & 0 \end{bmatrix} \begin{bmatrix} u \\ w \\ q \\ \theta \\ h \end{bmatrix} + \begin{bmatrix} X_{\delta_e} & X_{\delta_t} \\ Z_{\delta_e} & 0 \\ M_{\delta_e} & M_{\delta_t} \\ 0 & 0 \\ 0 & 0 \end{bmatrix} \begin{bmatrix} \delta_e \\ \delta_t \end{bmatrix} \tag{8}$$

As intuitively expected, the rank of the controllability matrix of this system using both controls is found to be **five** which ensures linear controllability of the fifth-order longitudinal flight dynamics model. A direct implication from the definition of controllability is that we can increase both velocity and altitude (i.e., no reliance on potential energy).

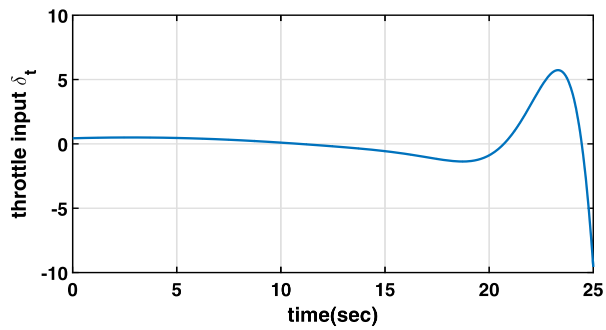

Fig. 5. Control input history for DELTA aircraft to reach $\boldsymbol{x}_1 = [80 \quad 0 \quad 0 \quad 3.7^\circ \quad 150]'$ using throttle only.

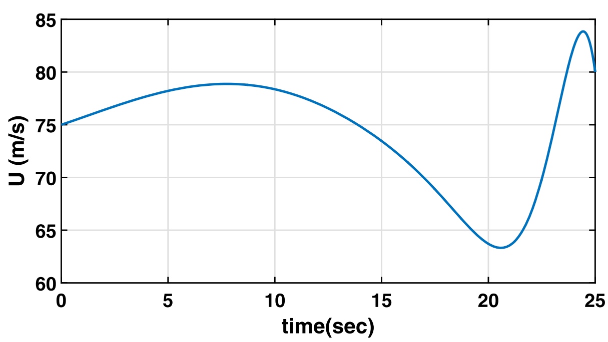

Fig. 6. Variation of the body velocity U for DELTA aircraft model due to the control input shown in Fig. 5.

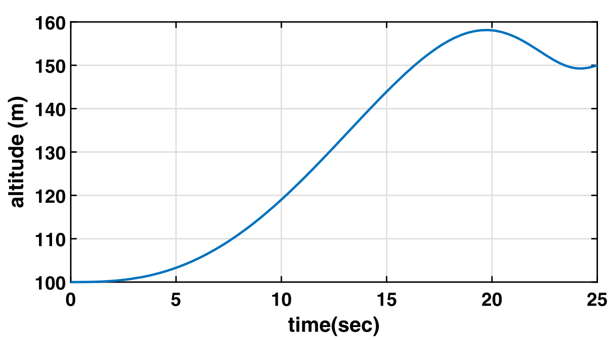

Fig. 7. Variation of the altitude h for DELTA aircraft model due to the control input shown in Fig. 5.

Now, assume that there is an elevator or an engine failure. Then the rank of the controllability matrix is found to be also **five**, which means that the system remains controllable. This may be intuitively acceptable for the case of elevator loss, but not in the case of engine loss. The existence of a control input history in this case can be verified as before using the control law in Eq. (3). Assume that the targeted state vector $\boldsymbol{x}_1$ is the same as the previous section with the desired altitude perturbation to be +50 m from the initial altitude which is assumed to be 100 m (i.e., $\boldsymbol{x}_1 = [80 \quad 0 \quad 0 \quad 3.7^\circ \quad 150]'$). Figs. 5–7 show the throttle control input history to reach the state $\boldsymbol{x}_1$ over the course of 25 seconds using throttle only, the resulting forward velocity U, and the resulting altitude h respectively.

For the case of throttle regulation loss, despite the fact that the controllability matrix is of full rank, the control input history required to reach $\boldsymbol{x}_1$ and the corresponding airplane simulated trajectory are found to be unrealistic as shown in Figs. 8, 9, and 10. This finding, which agrees with physical intuition, refutes the mathematical controllability consequent upon the satisfaction of the Kalman rank condition.

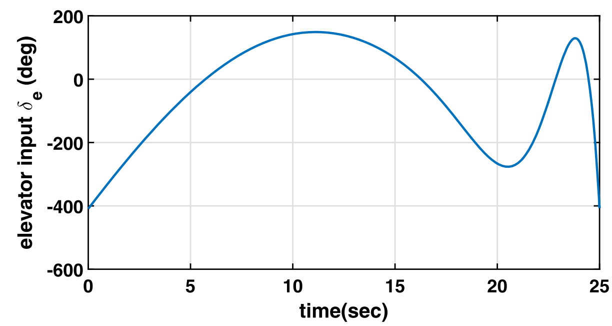

Fig. 8. Control input history for DELTA aircraft to reach $\boldsymbol{x}_1 = [80 \quad 0 \quad 0 \quad 3.7^\circ \quad 150]'$ using elevator only.

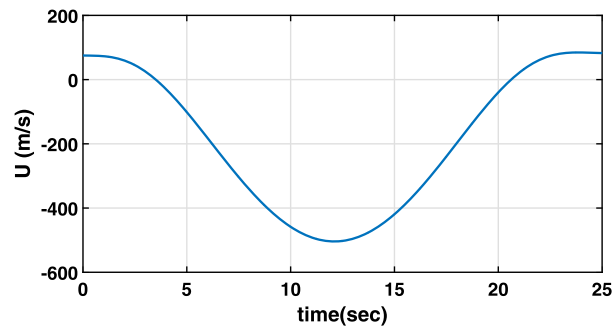

Fig. 9. Variation of the body velocity U for DELTA aircraft model due to the control input shown in Fig. 8.

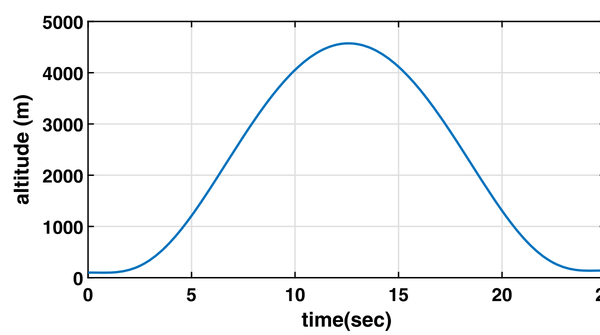

Fig. 10. Variation of the altitude h for DELTA aircraft model due to the control input shown in Fig. 8.

3.3. *Longitudinal* 6×6 *flight dynamics model*

In this subsection, the airplane's altitude h and north position coordinate P_N in the inertial frame are included in the longitudinal flight dynamics model and the controllability is assessed. Firstly, the full longitudinal flight dynamics model is written as

$$\begin{bmatrix} \dot{u} \\ \dot{w} \\ \dot{q} \\ \dot{\theta} \\ \dot{P}_N \\ \dot{h} \end{bmatrix} = \begin{bmatrix} X_u & X_w & 0 & -g\cos\theta_0 & 0 & 0 \\ Z_u & Z_w & U_0 & -g\sin\theta_0 & 0 & 0 \\ M_u & M_w & M_q & -gM_w\sin\theta_0 & 0 & 0 \\ 0 & 0 & 1 & 0 & 0 & 0 \\ \cos\theta_0 & \sin\theta_0 & 0 & -U_0\sin\theta_0 & 0 & 0 \\ \sin\theta_0 & -\cos\theta_0 & 0 & U_0\cos\theta_0 & 0 & 0 \end{bmatrix} \begin{bmatrix} u \\ w \\ q \\ \theta \\ P_N \\ h \end{bmatrix} + \begin{bmatrix} X_{\delta_e} & X_{\delta_t} \\ Z_{\delta_e} & 0 \\ M_{\delta_e} & M_{\delta_t} \\ 0 & 0 \\ 0 & 0 \\ 0 & 0 \end{bmatrix} \begin{bmatrix} \delta_e \\ \delta_t \end{bmatrix} \tag{9}$$

The rank of the controllability matrix of this system using both controls is found to be **six**. However, if either elevator control or throttle regulation is lost, the rank of the controllability matrix is found to be **five**, which means that the system is linearly uncontrollable. The practical implications of this finding can be understood in the context of a landing problem where the end point has specified coordinates P_N and h. The found uncontrollability of the system, if one controller fails, implies that some combination(s) of P_N and h may not be reached. However, since controllability of the linearization is only sufficient, the system may still be controllable and further nonlinear analysis is required [4,9,11,7,19,1].

This case worth more discussion. Full controllability of the longitudinal flight dynamics including navigation states is an overly stringent requirement that may not be needed. It should be noted that linear controllability (controllability of the linearized system) implies the ability to *locally* reach all neighboring points in all directions; that is, for example, to be able to move forward and backward. In fact, such an ability is not even guaranteed with full control authority because large negative thrust forces are not attainable for a conventional airplane. However, the Kalman rank condition assumes unbounded controls in all directions and, as such, did not show uncontrollability for the system (9) with full control authority (both elevator and thrust are functioning). This discussion invokes more relaxed notions for controllability. In fact, these notions already exist for nonlinear systems; *Accessibility* is a controllability notion for nonlinear systems that implies the ability to move in all neighboring directions, possibly in a biased manner. Formally, the accessibility property at $\boldsymbol{x}_0$ implies that the set $\mathcal{R}$ of reachable points from $\boldsymbol{x}_0$ has a non-empty interior. That is, an accessible system can be driven forward in some direction but not backward, which is similar to the expectations with the present example. Therefore, nonlinear analysis and controllability definitions are indeed invoked in such a case, which will be considered in detail in a successive effort.

3.4. Lateral 5 × 5 flight dynamics model

The lateral flight dynamics model of a rigid aircraft using the standard aileron and rudder controls along with a differential thrust control can be written as

$$\begin{bmatrix} \dot v \\ \dot p \\ \dot r \\ \dot\phi \\ \dot\psi \end{bmatrix} = \begin{bmatrix} Y_v & Y_p & -(U_0 - Y_r) & g\cos\theta_0 & 0 \\ \mathcal{L}_v & \mathcal{L}_p & \mathcal{L}_r & 0 & 0 \\ N_v & N_p & N_r & 0 & 0 \\ 0 & 1 & 0 & 0 & 0 \\ 0 & 0 & \sec\theta_0 & 0 & 0 \end{bmatrix} \begin{bmatrix} v \\ p \\ r \\ \phi \\ \psi \end{bmatrix} + \begin{bmatrix} 0 & Y_{\delta_r} & 0 \\ \mathcal{L}_{\delta_a} & \mathcal{L}_{\delta_r} & \mathcal{L}_{\delta_{t_d}} \\ N_{\delta_a} & N_{\delta_r} & N_{\delta_{t_d}} \\ 0 & 0 & 0 \\ 0 & 0 & 0 \end{bmatrix} \begin{bmatrix} \delta_a \\ \delta_r \\ \delta_{t_d} \end{bmatrix} \tag{10}$$

where v is the velocity of the airplane center of mass along the body starboard lateral axis, p and r are the roll and yaw rates, respectively, and ϕ and ψ are the corresponding Euler angles. The lateral controls include the aileron deflection δ_a, the rudder deflection δ_r and the differential thrust control δ_{t_d}. The latter represents asymmetric thrust variations from the cruise values, which mainly creates a yawing moment (in addition to a rolling moment in case of inertial cross coupling). The parameters Y_v, Y_p, Y_r, $\mathcal{L}_v$, $\mathcal{L}_p$, $\mathcal{L}_r$, N_v, N_p, N_r, Y_{δ_r}, $\mathcal{L}_{\delta_a}$, $\mathcal{L}_{\delta_r}$, $\mathcal{L}_{\delta_{t_d}}$, N_{δ_a}, N_{δ_r}, and $N_{\delta_{t_d}}$ are stability and control derivatives at the cruise condition.

The rank of the controllability matrix for this system is found to be **five** (i.e., fully controllable). In fact, the lateral dynamics is luxurious in controllability. That is, if we drop any two controls and retain only one, we find that the system remains linearly controllable. Moreover, this controllability is not affected if the airplane does not have inertial coupling (i.e., $J_{xz} = 0$), which weakens the roll-yaw coupling control derivatives N_{δ_a} and $\mathcal{L}_{\delta_r}$ and makes $\mathcal{L}_{\delta_{t_d}} = 0$. That is, the lateral flight dynamics can be controlled using only differential thrust even for zero-inertial coupling airplanes.

4. Application to thrust-only flight control system

As shown in the preceding sections, both longitudinal and lateral flight dynamics (excluding the navigation states) have been proved to be controllable using thrust inputs (symmetric and asymmetric) only. This invokes analyzing the emergency cases where there is a complete hydraulic failure during flight and consequently all the control surfaces are lost. In this section we will investigate the ability of a specific airplane to land safely using only the thrust control input without exceeding the control input bounds, i.e., maximum allowable thrust.

Consider the same airplane adopted before in Sec. 3, DELTA aircraft, at the same flight condition. To investigate the capability of this airplane to achieve safe landing-approach using thrust-control only, the criteria would be to achieve the appropriate flight path angle γ for the final approach, which is $-3°$ in most airports, and the appropriate approach speed V_T which is usually taken to be $1.3\ V_{stall}$. To take the effect of engine time lag into consideration we will represent the engine dynamics as a first order system with time constant $T = 10$ seconds. As such, the transfer function of the engine dynamics can be written as

$$\frac{\delta_t}{e_{\delta_t}} = \frac{0.1}{s + 0.1} \tag{11}$$

where e_{δ_t} is the input signal to the engine (e.g., a throttle lever displacement). As such, the engine time-lag is written in a state space form as

$$\dot\delta_t = -0.1\delta_t + 0.1 e_{\delta_t} \tag{12}$$

Combining the engine-dynamics as represented by Eq. (12) into the longitudinal flight dynamics (7), we write

$$\begin{bmatrix} \dot u \\ \dot w \\ \dot q \\ \dot\theta \\ \dot\delta_t \end{bmatrix} = \begin{bmatrix} X_u & X_w & 0 & -g\cos\theta_0 & X_{\delta_t} \\ Z_u & Z_w & U_0 & -g\sin\theta_0 & 0 \\ M_u & M_w & M_q & -gM_w\sin\theta_0 & M_{\delta_t} \\ 0 & 0 & 1 & 0 & 0 \\ 0 & 0 & 0 & 0 & -0.1 \end{bmatrix} \begin{bmatrix} u \\ w \\ q \\ \theta \\ \delta_t \end{bmatrix} + \begin{bmatrix} 0 \\ 0 \\ 0 \\ 0 \\ 0.1 \end{bmatrix} e_{\delta_t} \tag{13}$$

To track the desired flight path angle during landing-approach using TFCS, we use a linear-state-feedback servo-mechanism. That is, we use the control law

$$\begin{aligned} u_c(t) &= -\boldsymbol{k}\,\boldsymbol{x}(t) + k_i\, e(t) \\ \dot e(t) &= r - y(t) \end{aligned} \tag{14}$$

where $u_c(t)$ is the control input, $\boldsymbol{x}(t)$ is the state vector, the output (flight path angle in this case) $y = \boldsymbol{C}\boldsymbol{x}$, $\boldsymbol{k}$ is the (1×5) state-feedback gain matrix, and k_i is an integral gain. The servo-mechanism induces an additional state variable e whose rate represents the error between the desired reference and output signals. As such, feeding back by this state represents an integral control action that eliminates steady state error. The full system dynamics (when $r = 0$) is then written as

$$\begin{bmatrix} \dot{\boldsymbol{x}} \\ \dot{e} \end{bmatrix} = \begin{bmatrix} \boldsymbol{A} & 0 \\ -\boldsymbol{C} & 0 \end{bmatrix} \begin{bmatrix} \boldsymbol{x} \\ e \end{bmatrix} + \begin{bmatrix} \boldsymbol{B} \\ 0 \end{bmatrix} u_c$$
$$y = \begin{bmatrix} \boldsymbol{C} & 0 \end{bmatrix} \begin{bmatrix} \boldsymbol{x} \\ e \end{bmatrix} \tag{15}$$

where $\boldsymbol{A}$, $\boldsymbol{B}$, and $\boldsymbol{C}$ are the matrices of the original 5×5 longitudinal system shown in Eq. (13). The closed loop system can be written as

$$\begin{bmatrix} \dot{\boldsymbol{x}} \\ \dot{e} \end{bmatrix} = \begin{bmatrix} \boldsymbol{A} - \boldsymbol{B}\boldsymbol{k} & \boldsymbol{B}k_i \\ -\boldsymbol{C} & 0 \end{bmatrix} \begin{bmatrix} \boldsymbol{x} \\ e \end{bmatrix} + \begin{bmatrix} 0 \\ 0 \\ 0 \\ 0 \\ 0 \\ 1 \end{bmatrix} r$$
$$y = \begin{bmatrix} \boldsymbol{C} & 0 \end{bmatrix} \begin{bmatrix} \boldsymbol{x} \\ e \end{bmatrix}. \tag{16}$$

To solve for the state-feedback gains ($\boldsymbol{k}$ and k_i), we formulate a linear quadratic regulator (LQR) problem; that is, we consider the quadratic cost function

$$J = \int_0^\infty (\boldsymbol{x}^T \boldsymbol{Q}\, \boldsymbol{x} + \boldsymbol{u}^T \boldsymbol{R} \boldsymbol{u}) dt \tag{17}$$

where, in this case, $\boldsymbol{x}$ is the augmented state vector $[\boldsymbol{x} \quad e]'$ and $\boldsymbol{u}$ is the control input u_c. We consider the weighting matrices $\boldsymbol{Q}$ and $\boldsymbol{R}$ to be in the form

$$\boldsymbol{Q} = \begin{bmatrix} \frac{1}{x_{1max}^2} & 0 & \dots & 0 \\ 0 & \frac{1}{x_{2max}^2} & \dots & 0 \\ \vdots & & \ddots & \vdots \\ 0 & \dots & \dots & \frac{1}{x_{nmax}^2} \end{bmatrix},$$
$$\boldsymbol{R} = \begin{bmatrix} \frac{1}{u_{1max}^2} & 0 & \dots & 0 \\ 0 & \frac{1}{u_{2max}^2} & \dots & 0 \\ \vdots & & \ddots & \vdots \\ 0 & \dots & \dots & \frac{1}{u_{mmax}^2} \end{bmatrix} \tag{18}$$

where $x_{i_{max}}$ is the desired maximum allowable perturbation for the state variable x_i and $u_{j_{max}}$ is the physical limit imposed on the control input u_j. The resulting controller guarantees the asymptotic stability of the dynamics (16) for any constant r. For more details about LQR controller design, the reader is referred to [10]. In our case, there is only one control input e_{δ_t}, so the $\boldsymbol{R}$ matrix will be reduced to the scalar $\frac{1}{e^2_{\delta_{tmax}}}$. According to the thrust trim value T_{trim} and the control derivatives X_{δ_t} and M_{δ_t} calculated in Sec. 3, the allowed δ_t should be between 1 and -0.56, then $\delta_{t_{max}} = e_{\delta_{t_{max}}}$ is chosen to be 0.56 (note the unity dc gain between e_{δ_t} and δ_t). The maximum allowable perturbations for the states are chosen to be $u_{max} = 5$ m/s, $w_{max} = 2$ m/s, $q_{max} = 2$ deg/s, and $\theta_{max} = 10°$.

4.1. Regulation of the flight path angle during landing-approach

To track a $-3°$ step reference signal for the flight path angle, we define $y = \gamma = \boldsymbol{C}\boldsymbol{x}$ with $\boldsymbol{C} = [0 \ \ \frac{-1}{U_0} \ \ 0 \ \ 1 \ \ 0]$. Using the LQR problem formulation shown above, the appropriate gains can be calculated, the closed-loop system is simulated over the course of 100 seconds and the resulting flight path angle and throttle input are shown in Figs. 11 and 12 respectively. It is interesting to note that the desired flight path angle for landing-approach can be ensured using a TFCS without exceeding the throttle control input bounds even if engine lag is included.

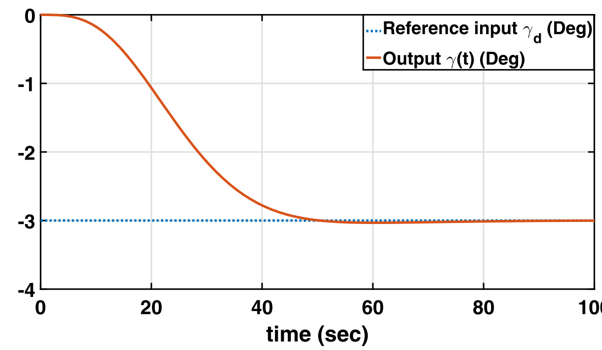

Fig. 11. Closed loop response of the flight path angle γ due to a $-3°$ step reference input using the designed LQR servo system.

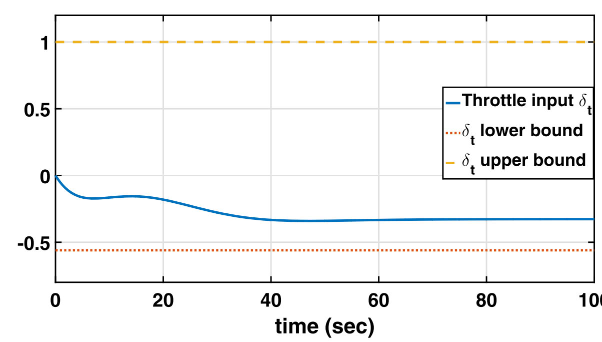

Fig. 12. Required engine throttle manipulation to ensure a flight path angle $\gamma = -3°$ using the designed LQR servo system.

4.2. Analysis of the raised concerns about TFCS

4.2.1. Lack of pitch control authority when $M_{\delta_t} = 0$

An intuitive concern raised by Lemaignan [13] is that a zero thrust-line-cg offset ($M_{\delta_t} = 0$) might preclude pitch controllability and, as such, the landing-approach could not be performed using thrust-only. However, our current analysis shows that regulation of the flight path angle for landing-approach is achievable using a TFCS even if $M_{\delta_t} = 0$. In fact, we find very similar responses in the case of $M_{\delta_t} = 0$ to those shown in Figs. 11 and 12 with the steady state value of δ_t is slightly higher.

4.2.2. Inability to regulate both flight path angle and speed during landing-approach

In reality, landing is one of the most intricate flight conditions, if not the most. It does not only require regulation of the flight path angle but also the flight speed. Regulation of the flight speed can be easily achieved using a TFCS. However, we find that, similar to Lemaignan's conclusion [13], simultaneous regulation for γ and V_T is not possible using a TFCS, which is physically intuitive. As such, in such an emergency case where a TFCS is used, the airplane will have to land at a speed higher than the standard requirements ($1.3\ V_{stall}$).

4.2.3. Effect of engine time lag on yaw damping

A legitimate concern raised by Nguyen et al. [16] is that while airplane controllability may still be ensured using TFCSs, the time lag associated with engine dynamics might affect stabilization of the lateral flight dynamics. In particular, the use of differential thrust inputs might not be effective in damping the Dutch roll mode because the engine dynamics will not be fast

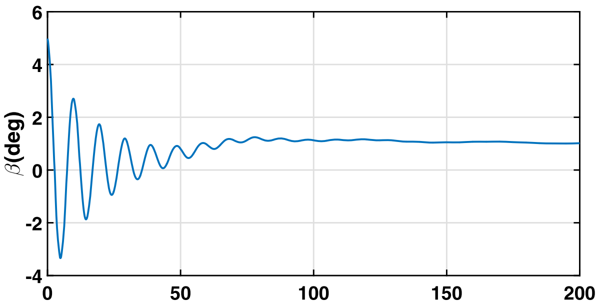

(a) Side-slip angle β

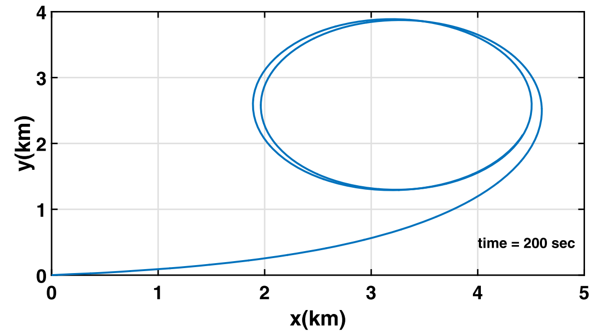

(b) Horizontal trajectory in the inertial frame

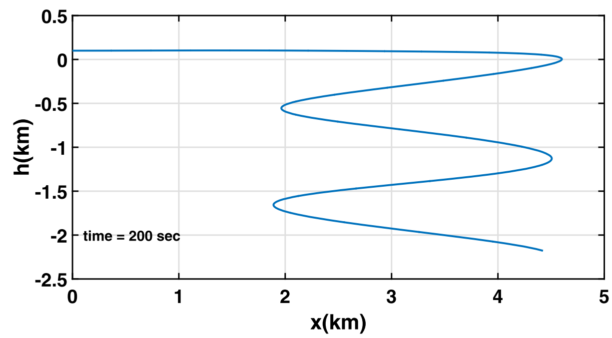

(c) Vertical trajectory in the inertial frame

Fig. 13. Airplane open loop response due to 5° side-slip disturbance.

enough to recover the airplane from a side-slip disturbance before getting into an unrecoverable upset situation. In this subsection, we investigate the effect of the engine dynamics on yaw damping. We consider the lateral characteristics of DELTA aircraft model [14, pp. 561–563] at the flight condition (sea-level cruising at $U_0 = 75$ m/s and $\theta_0 = \alpha_0 = 2.7°$):

$$Y_v = -0.078,\ Y_p = 0,\ Y_r = 0,$$

$$\mathcal{L}_v = -0.0086,\ \mathcal{L}_p = -1.0758,\ \mathcal{L}_r = 0.6334,$$

$$N_v = 0.0037,\ N_p = -0.1121,\ N_r = -0.2569,$$

$$\mathcal{L}_{\delta_{t_d}} = 0.0031,\ N_{\delta_{t_d}} = 0.0345.$$

To make our investigation more relevant to the raised point, we decrease the yaw damping derivative N_r of the airplane to be 20% of the original value. Also, we consider the full 12×12 nonlinear model, developed earlier [8] for simulation to account for the longitudinal–lateral coupling, which may result in an upset situation due to a side-slip disturbance. Fig. 13 shows the open loop response of the DELTA aircraft (with $N_r = -0.0514$) due to a 5° side slip disturbance. Clearly, the airplane goes into a spiral dive.

We then design a simple yaw damper using rudder input as $\delta_r = -kr$. The closed loop response due to a 5° side slip disturbance is shown in Fig. 14. As expected, the yaw damper is very efficient in damping the side slip disturbance. Now, we assume that the rudder control authority is lost and we only rely on a TFCS. We design the following yaw damper $e_{\delta_{t_d}} = -k\ r$ and simulate the full 12×12 system in addition to the engine lag dynamics (12). Fig. 14 provides a comparison between the response of the two closed loop systems; using rudder and differential thrust. While the response using the TFCS is more sluggish than that of the rudder, it is quite acceptable and the airplane did not diverge into any upset situation, even in the presence of a considerable engine lag. It should be noted that TFCS are not meant to replace the conventional primary flight controls but to be used in emergency situations. This analysis shows its efficacy in such situations.

5. Conclusions

In this work, a linear controllability approach is adopted to study airplane flight dynamics in different loss-of-control situations using different model sizes. For the conventional fourth-order longitudinal flight dynamics, we show that the system remains controllable if the elevator control input or the throttle regulation is lost. However, the elevator-only longitudinal controller relies on the available gravitational potential energy. To prevent such an exploitation, we added the altitude to the state variables and found that the resulting fifth-order longitudinal flight dynamics cannot be controlled using elevator only but is still controllable using thrust only. If all longitudinal kinematic variables are included (i.e., sixth-order flight dynamic model), linear controllability becomes deficient if either elevator or throttle is lost. In such a case, nonlinear controllability analysis is discussed and invoked because of its relaxed notions of controllability. On the other hand, the conventional fifth-order lateral flight dynamics is shown to be controllable using either aileron or rudder controls. Moreover, both aileron and rudder could be replaced with a differential thrust control input without diminishing linear controllability. We also stress the fact the system being controllable using only one controller does not guarantee equilibrium at the end state; i.e., the system may depart from such a state immediately after the excursion time.

In this work, we also considered application of the linear controllability analysis to Thrust-only Flight Control Systems (TFCSs). We show that the desired flight path angle for landing-approach can be tracked using a TFCS without exceeding the thrust control input bounds even if the engine lag is considered. Then, we address some of the previously raised concerns about TFCSs. Firstly, we show that flight path angle regulation during the landing-approach is also achievable using TFCS even if $M_{\delta_t} = 0$. Secondly, we confirm the previously raised issue that is both flight path angle and speed cannot be simultaneously regulated using TFCS during the landing-approach. Thirdly, we investigate the effect of slow engine dynamics on yaw damping in the case of rudder loss.

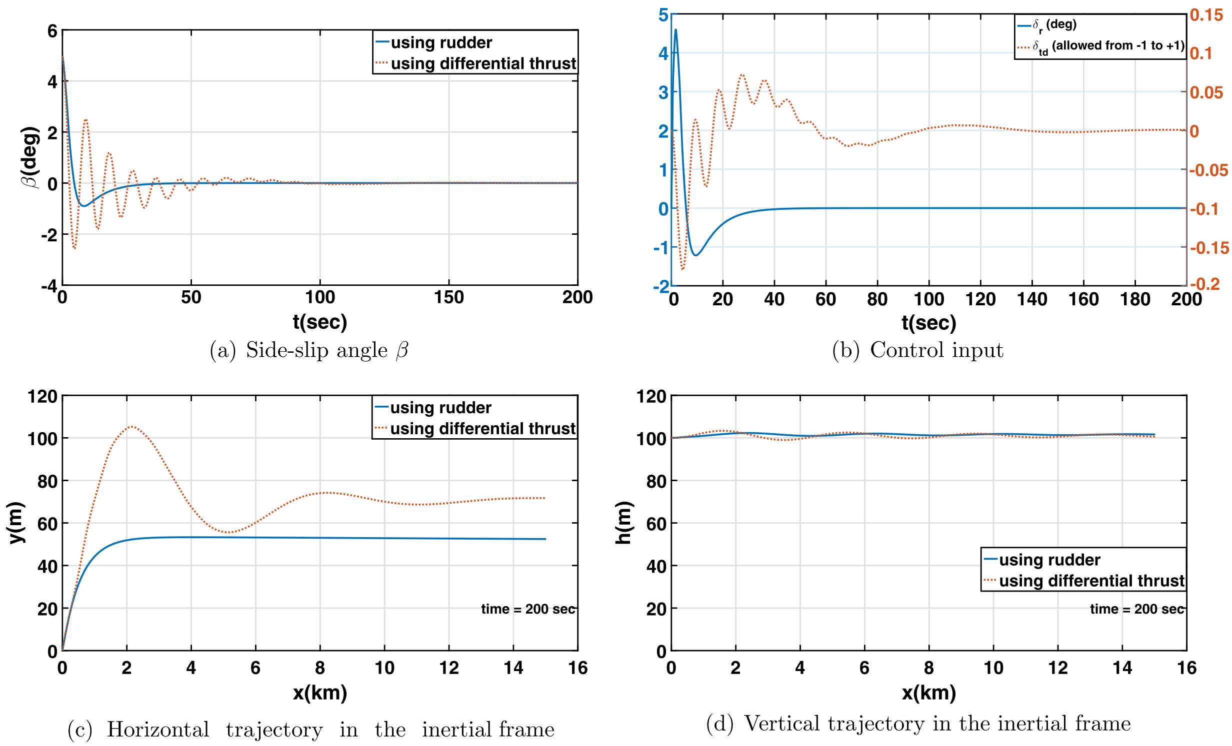

(a) Side-slip angle β

(b) Control input

(c) Horizontal trajectory in the inertial frame

(d) Vertical trajectory in the inertial frame

Fig. 14. Airplane closed loop response due to 5° side-slip disturbance.

We conclude that differential thrust control represents a practical solution for lateral stabilization and control in case of aileron and rudder failure, even with a slow engine dynamics and unstable open loop flight dynamics. Finally, we conclude by proposing use of nonlinear controllability to analyze the linearly uncontrollable situations and assess potential exploitation of nonlinear interacting mechanisms to enhance controllability. This point will be considered in future by the authors.

Conflict of interest statement

There is no conflict of interest.

References

[1] R.M. Bianchini, G. Stefani, Graded approximations and controllability along a trajectory, SIAM J. Control Optim. 28 (4) (1990) 903–924.
[2] J.H. Blakelock, Automatic Control of Aircraft and Missiles, John Wiley & Sons, 1991.
[3] R.W. Brockett, Finite Dimensional Linear Systems, Wiley, New York, 1970.
[4] P. Brunovsky, Local controllability of odd systems, in: Banach Center Publ., vol. 1, 1974, pp. 39–45.
[5] F.W. Burcham, J. Burken, T.A. Maine, Flight testing a propulsion-controlled aircraft emergency flight control system on an F-15 airplane, National Aeronautics and Space Administration, Office of Management, Scientific and Technical Information Program, 1994.
[6] F.W. Burcham, T.A. Maine, J.J. Burken, Development and flight test of an augmented thrust-only flight control system on an MD-11 transport airplane, National Aeronautics and Space Administration, Office of Management, Scientific and Technical Information Program, 1996.
[7] P.E. Crouch, C.I. Byrnes, Local accessibility, local reachability, and representations of compact groups, Math. Syst. Theory 19 (1) (1986) 43–65.
[8] A.M. Hassan, H.E. Taha, Geometric nonlinear controllability analysis for airplane flight dynamics, in: Proc. AIAA SciTech., 2016.
[9] H. Hermes, On local controllability, SIAM J. Control Optim. 20 (2) (1982) 211–220.
[10] J.P. Hespanha, Linear Systems Theory, Princeton University Press, 2009.
[11] V. Jurdjevic, Polynomial control systems, in: Proc. 22nd IEEE CDC, vol. 2, 1983, pp. 904–906.
[12] H.G. Kwatny, J.-E.T. Dongmo, B.-C. Chang, G. Bajpai, M. Yasar, C. Belcastro, Nonlinear analysis of aircraft loss of control, J. Guid. Control Dyn. 36 (1) (2012) 149–162.
[13] B. Lemaignan, Flying with no flight controls: handling qualities analyses of the Baghdad event, in: AIAA Atmospheric Flight Mechanics Conference, 2005, AIAA-2005-5907.
[14] D. McLean, Automatic Flight Control Systems, Prentice Hall, 1990.
[15] R.C. Nelson, Flight Stability and Automatic Control, 2nd edition, McGraw-Hill, 1998.
[16] N. Nguyen, K. Krishnakumar, J. Kaneshige, P. Nespeca, Dynamics and adaptive control for stability recovery of damaged asymmetric aircraft, in: AIAA Guidance Navigation and Control Conference, Keystone, CO, 2006.
[17] H. Nijmeijer, A. Van der Schaft, Nonlinear Dynamical Control Systems, Springer Science & Business Media, 1990.
[18] R.E. Kalman, Y.C. Ho, K.N. Narendra, Controllability of linear dynamical systems, Contrib. Differ. Equ. 1 (1963) 189–213.
[19] H.J. Sussmann, A general theorem on local controllability, SIAM J. Control Optim. 25 (1) (1987) 158–194.
[20] T. Tucker, Touchdown: the development of propulsion controlled aircraft at NASA dryden, NASA History Office, Office of Policy and Plans, NASA Headquarters, 1999.
[21] J.E. Wilborn, J.V. Foster, Defining commercial transport loss-of-control: a quantitative approach, in: AIAA Atmospheric Flight Mechanics Conference and Exhibit, 2004, p. 4811.
[22] K. Yamasaki, Y. Ichihara, H. Yasui, S. Hiranuma, A thrust-only flight-control system as a backup for loss of primary flight controls, Mitsubishi Heavy Industries Tech. Rev 48 (4) (2011) 1.